European Journal of Medicinal Chemistry 45 (2010) 4358–4364

Contents lists available at ScienceDirect

European Journal of Medicinal Chemistry

journal homepage: http://www.elsevier.com/locate/ejmech

Short communication

Design and synthesis of potent inhibitors of β-ketoacyl-acyl carrier protein synthase III (FabH) as potential antibacterial agents

Lei Shi [a], Rui-Qin Fang [a], Zhen-Wei Zhu [a], Ying Yang [a], Kui Cheng [a], Wei-Qing Zhong [b,*], Hai-Liang Zhu [a,*]

[a] State Key Laboratory of Pharmaceutical Biotechnology, Nanjing University, Nanjing 210093, PR China
[b] School of Pharmacy, Second Military Medical University, Shanghai 200433, PR China

ARTICLE INFO

Article history:
Received 26 August 2009
Received in revised form
7 December 2009
Accepted 14 May 2010
Available online 24 May 2010

Keywords:
FabH
Inhibitor
Antibacterial
Structure–activity relationship
Schiff base

ABSTRACT

Twenty new Schiff bases were synthesized by reacting 5-fluoro-salicylaldehyde and primary amine as potent inhibitors of FabH. These compounds were assayed for antibacterial activity against *Escherichia coli*, *Pseudomonas fluorescence*, *Bacillus subtilis* and *Staphylococcus aureus*. Compounds with potent antibacterial activities were tested for their *E. coli* FabH inhibitory activity. (*E*)-4-fluoro-2-((4-hydroxyphenethylimino)methyl)phenol (**10**) showed the most potent antibacterial activity with MIC of 1.56–6.25 μg/mL against the tested bacterial strains and exhibited the most potent *E. coli* FabH inhibitory activity with IC_{50} of 2.7 μM. Docking simulation was performed to position compound **10** into the *E. coli* FabH active site to determine the probable binding conformation.

1. Introduction

Although several classes of antibacterial agents are presently available, resistance in most of the pathogenic bacteria to these drugs constantly emerges. In order to prevent this serious medical problem, the elaboration of new types of antibacterial agents or the expansion of bioactivity of the previous drugs is a very important task [1]. Therefore, in recent years, the research has been focused toward development of new antibacterial agents, which may act through novel target, surpassing the problem of acquired resistance.

A promising target is the fatty acid synthase (FAS) pathway in bacteria. Fatty acid biosynthesis (FAB) is an essential metabolic process for prokaryotic organisms and is required for cell viability and growth [2]. Large multifunctional proteins termed type I fatty acid synthases (FAS I) catalyze these essential reactions in eukaryotes [3–5]. In contrast, bacteria use multiple enzymes to accomplish the same goal and are referred to as type II, or dissociated, fatty acid synthases (FAS II) [6,7]. β-Ketoacyl-acyl carrier protein (ACP) synthase III, also known as FabH or KAS III, plays an essential and regulatory role in bacterial FAB [8,9]. The enzyme initiates the fatty acid elongation cycles [10,11], and is involved in the feedback regulation of the biosynthetic pathway via product inhibition [12]. FabH catalyzes the condensation reaction between a CoA-attached acetyl group and an ACP-attached malonyl group, yielding acetoacetyl-ACP as its final product (Fig. 1). Two other condensing enzymes, FabB (KAS I) and FabF (KAS II), perform the chain elongation reactions in subsequent cycles leading to long-chain acyl ACP products [6,8], while FabB and FabF are also condensing enzymes, FabH is structurally distinct.

FabH proteins from both Gram-positive and Gram-negative bacteria are highly conserved at the sequence and structural level while there are no significantly homologous proteins in humans. Importantly, the residues that comprise the active site are essentially invariant in various bacterial FabH molecules [13–15]. FabH represents a promising target for the design of novel antimicrobial drugs, since it regulates the fatty acid biosynthesis rate via an initiation pathway and its substrate specificity is a key factor in membrane fatty acid composition [16–18]. These attributes suggest that small molecule inhibitors of FabH enzymatic activity could be potential development candidates leading to selective, nontoxic, and broad-spectrum antibacterials.

Various kinds of compounds were screened by enzymatic assays to generate leads that were co-crystallized with various pathogenic FabH proteins and subsequently optimized using structure guided drug design methods [19–23]. Y. Kim and coworkers reported the YKAs3003, a Schiff base condensed by 4-hydroxy salicylaldehyde and cyclohexanamine as a potent inhibitor of *Escherichia coli* (*E. coli*) FabH with antimicrobial activity [24]. Further optimization

* Corresponding author. Tel.: +86 25 8359 2572; fax: +86 25 8359 2672.
E-mail address: zhuhl@nju.edu.cn (H.-L. Zhu).

0223-5234/$ – see front matter © 2010 Elsevier Masson SAS. All rights reserved.
doi:10.1016/j.ejmech.2010.05.033

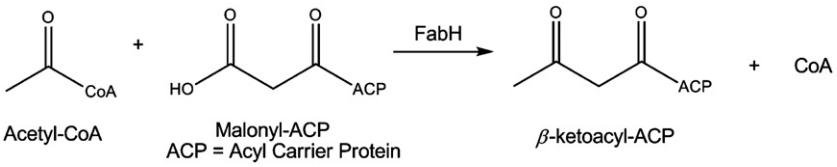

Fig. 1. FabH-catalyzed initiation reaction of fatty acid biosynthesis.

of this compound is required to improve its antimicrobial activity. It was well known that some fluoro-substituted organic substances, such as norfloxacin, ciprofloxacin, levofloxacin, linezolid, exhibited favorable antibacterial activities because fluorin atom may play an important role in improving the pharmacokinetics properties of the compounds [25–28]. In this study, we designed and synthesized a new series of Schiff bases derived from 5-fluoro-salicylaldehyde and studied their antibacterial activities and *E. coli* FabH inhibitory activities. Docking simulations were performed using the X-ray crystallographic structure of the FabH of *E. coli* in complex with the most potent inhibitor to explore the binding modes of these compounds at the active site.

2. Results and discussion

2.1. Chemistry

In the present study, 20 primary amines were respectively subjected to react with 5-fluoro-salicylaldehyde to prepare the corresponding Schiff bases (Scheme 1). All the compounds gave satisfactory chemical analyses (±0.4%). ^{1}H NMR and ESI-MS spectra were consistent with the assigned structures. Compound **10** was successfully crystallized and its structure was determined by single-crystal X-ray diffraction analysis. Fig. 2 gives a perspective view of this compound together with the atomic labeling system. In the structure of compound **10**, all bond lengths are within normal ranges [29]. The bond length between C7 and N1 (1.284 Å) conform to the value for a carbon-nitrogen double bond, while the bond length between C8 and N1 (1.463 Å) conform to the value for a carbon-nitrogen single bond. The bond length of C2–O1 (1.302 Å) is shorter than C13–O1 (1.363 Å) because of the existence of the hydrogen bond (O2–H2…N1: 2.565(3) Å, 149.5°). There is an intermolecular O–H…O hydrogen bond (O1–H1…O2: 2.707(3) Å, 172.1°, Symmetry codes: −x + 1/2, y + 1/2, −z + 1/2) in the structure. The dihedral angle between the two benzene rings is 14.22 (0.21)°.

2.2. Biological activity

2.2.1. Antibacterial activity

All the synthesized compounds were screened for antibacterial activity against two Gram-negative bacterial strains: *E. coli* (*E. coli*) and *Pseudomonas fluorescence* (*P. fluorescence*) and two Gram-positive bacterial strains: *Bacillus Subtilis* (*B. Subtilis*) and *Staphylococcus aureus* (*S. aureus*) by MTT method. The MICs (minimum inhibitory concentrations) of the compounds against these bacteria were presented in Table 1. Also included was the activity of reference compounds kanamycin. The results revealed that most of the synthesized compounds exhibited significant antibacterial activities.

Out of the 20 synthetic new Schiff bases, compound **10**, (*E*)-4-fluoro-2-((4-hydroxyphenethylimino)methyl)phenol, exhibited the most potent antibacterial activity with MIC of 1.56, 3.13, 6.25 and 1.56 μg/mL against *E. coli*, *P. fluorescence*, *B. Subtilis* and *S. aureus*, respectively, which was similar to the broad-spectrum antibiotic kanamycin with corresponding MIC of 3.13, 3.13, 1.56 and 1.56 μg/mL.

The structure of compound **2**, (*E*)-4-fluoro-2-((cyclohexylimino)methyl)phenol was very similar to 4-cyclohexyliminomethyl-benzene-1,3-diol (YKAs3003) [24]. The difference between them is that 4-substituent of YKAs3003 is −OH while the 5-substituent of compound **2** is −F. However, compound **2** showed much more potent antibacterial activity than YKAs3003. The MIC of compound **2** against *E. coli*, *P. fluorescence*, *B. Subtilis* and *S. aureus* was 6.25, 12.5, 25 and 12.5 μg/mL, respectively while the MIC of YKAs3003 against *E. coli* and *S. aureus* was 128 and 256 μg/mL. This result suggested that the introduction of fluoro substituent increased the hydrophobicity of Schiff base and lead to the increase of the antibacterial activity and the location of substituent may also influence the activity. Compounds **1** and **3** with cyclopentyl and methyl-cyclohexyl substituent replacing the cyclohexyl substituent of compound **2** exhibited similar antibacterial activity to compound **2** with the MIC of 6.25–25 μg/mL against the tested bacterial strains.

Compounds **4** and **6** showed similar moderate antibacterial activity with MIC of 12.5–50 μg/mL against all the tested bacterial strains. This indicated that the introduction of morpholine or piperazine substituent cannot enhance the inhibitory activity obviously.

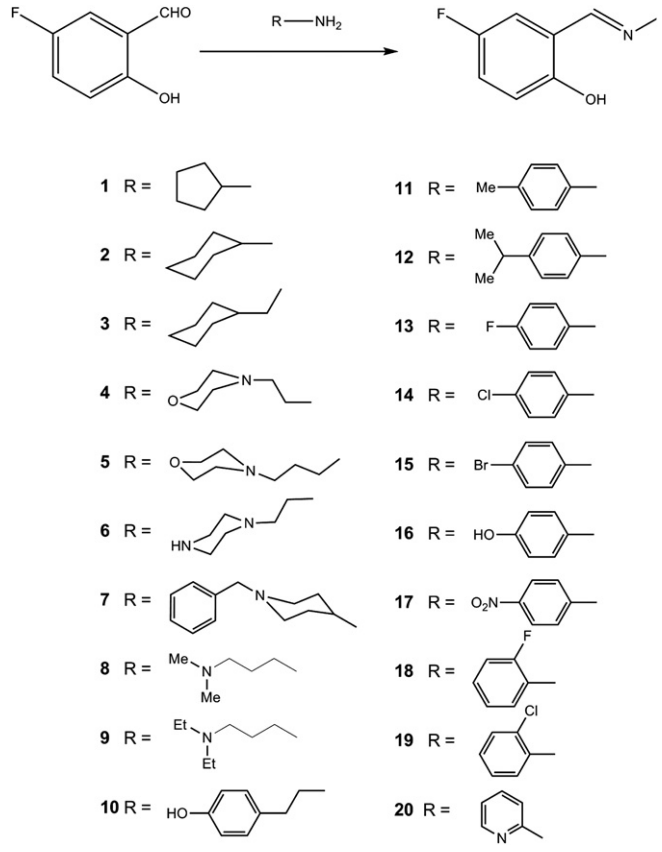

Scheme 1. Syntheses of the Schiff bases derived from 5-fluoro-salicylaldehyde.

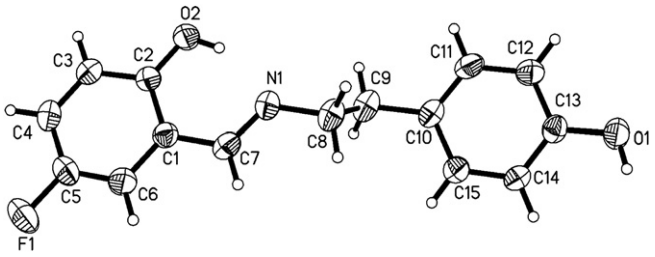

Fig. 2. Molecular structure of compound **10** with all atoms labeling. Displacement ellipsoids are drawn at the 30% probability level and H atoms are shown as small spheres of arbitrary radii.

Compounds **5**, **7**, **8** and **9** were found to be inactive against all the tested bacterial strains. This indicated that the introduction of long aliphatic chain lead to the decrease of antibacterial activity.

Compounds **11**–**19** were condensed by 5-fluoro-salicylaldehyde and substituted anilines. Various substituents of anilines such as hydroxyl, halogen and saturated alkyl lead to the different antibacterial activities of these Schiff bases. Compounds **18** and **19** with *o*-substituted fluoro and chloro group on aniline component showed significant antibacterial activity with MIC of 6.25–12.5 μg/mL against the tested bacterial strains. Compounds **13**–**15** with *p*-substituted halogen group on aniline component exhibited moderate activity with MIC of 12.5–50 μg/mL. These results demonstrated that the synthetic Schiff bases with *o*-substituted halogen group on aniline component showed slightly more potent antibacterial activity than that of *p*-substituted. The antibacterial activity of these compounds enhanced slightly in the order of substituent on aniline component: Br < Cl < F. We proposed that hydrophobic and electron-withdrawing halogen groups on aniline component were conducive to the antibacterial activity. Compounds **16** and **17** with hydroxyl and nitro substituent on aniline component were not active against all the tested bacterial strains. This indicated that hydrophilic groups on aniline component were not conducive to the antibacterial activity. Compounds **11** and **12** with methyl and isopropyl substituent on aniline component showed weak antibacterial activity with the MIC ranged from 50 to more than 100 μg/mL. This suggested that the electron-donating groups on aniline component were not favorable for activity. Compound **20** was condensed by 5-fluoro-salicylaldehyde and 2-aminopyridin and showed weak antibacterial activity.

Table 1
Antibacterial activity of synthetic compounds.

Compounds	Minimum inhibitory concentrations (μg/mL)			
	Gram-negative		Gram-positive	
	E. coli	*P. fluorescence*	*B. subtilis*	*S. aureus*
1	12.5	12.5	25	25
2	6.25	12.5	25	12.5
3	6.25	6.25	12.5	25
4	25	25	50	50
5	>100	>100	>100	>100
6	12.5	25	50	25
7	>100	>100	>100	>100
8	>100	>100	>100	>100
9	>100	>100	>100	>100
10	1.56	3.13	6.25	1.56
11	50	50	>100	100
12	>100	100	>100	>100
13	12.5	12.5	25	12.5
14	12.5	25	50	25
15	25	25	50	50
16	>100	>100	>100	>100
17	>100	>100	>100	>100
18	6.25	6.25	12.5	6.25
19	6.25	12.5	12.5	12. 5
20	50	100	>100	100
Kanamycin	3.13	3.13	1.56	1.56

2.2.2. *E. coli* FabH inhibitory activity

The *E. coli* FabH inhibitory potency of the synthetic Schiff bases with potent antibacterial activities (**1**–**3**, **6**, **10**, **13**, **14**, **18** and **19**) was examined and the results are summarized in Table 2. Most of the tested compounds displayed potent *E. coli* FabH inhibitory. Among them, compound **10** condensing by 5-fluoro-salicylaldehyde and tyramine showed the most potent inhibitory with IC_{50} of 2.7 μM. This result supported the potent antibacterial activities of **10**. It also indicated that the introduction of fluoro substituent and tyramine increased the inhibitory activity of Schiff bases. Compounds **1**–**3** with similar structure to YKAs3003 exhibited good inhibitory with IC_{50} ranged from 6.8 to 18.4 μM, which indicating that hydrophobic cyclopentyl and cyclohexyl substituent were favorable for the *E. coli* FabH inhibitory activity. Compounds **18** and **19** with *o*-substituted fluoro and chloro group on aniline component showed better *E. coli* FabH inhibitory activity than compounds **13** and **14** with *p*-substituted halogen group on aniline component. The results of *E. coli* FabH inhibitory activity of the test compounds were corresponding to the structure relationships (SAR) of their antibacterial activities. This demonstrated that the potent antibacterial activities of the synthetic compounds were probably correlated to their FabH inhibitory activities.

2.3. Binding model of compound ***10*** and *E. coli* FabH

Molecular docking of compound **10** and *E. coli* FabH was performed on the binding model based on the *E. coli* FabH–CoA complex structure (1HNJ.pdb) [30]. The FabH active site generally contains a catalytic triad tunnel consisting of Cys-His-Asn, which is conserved in various bacteria. This catalytic triad plays an important role in the regulation of chain elongation and substrate binding. Since the alkyl chain of CoA is broken by Cys of the catalytic triad of FabH, interactions between Cys and substrate appear to play an important role in substrate binding. Qiu, X. et al. have refined three-dimensional structure of *E. coli* FabH in the presence and absence of malonyl-CoA by X-ray spectroscopy. Since malonyl moiety is degraded by *E. coli* FabH, molecular docking studies for FabH and malonyl-CoA was carried out to identify a plausible malonyl-binding mode [30]. They found that in one of the binding modes appeared in the lower scored conformations, the malonyl carboxylate formed hydrogen bonds to the backbone nitrogen of Phe304.

The binding model of compound **10** and *E. coli* FabH is depicted in Fig. 3. In the binding model, amino hydrogen of Asn247 forms hydrogen bond with phenolic O1 of compound **10** (2.024 Å, 172.165°). There is a π–π interaction between the benzyl ring of compound **10** (C10, C11, C12, C13, C14, C15) and the benzyl ring of

Table 2
E. coli FabH inhibitory activity of synthetic compounds.

Compound	IC50 (μM)
1	18.4
2	7.4
3	6.8
6	48.5
10	2.7
13	28.6
14	42.5
18	8.6
19	11.7

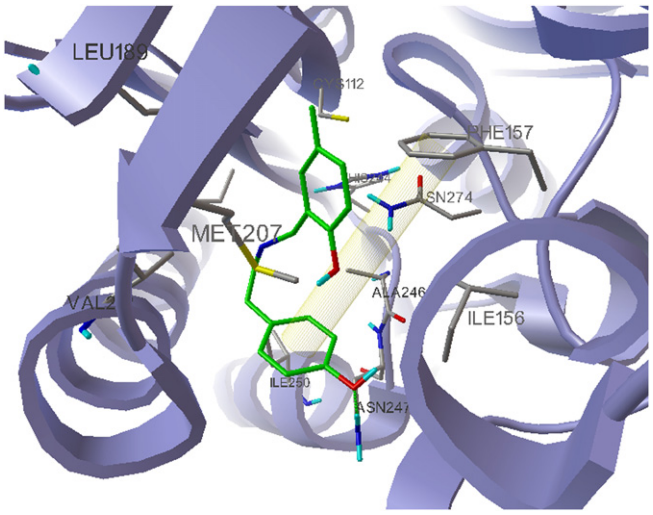

Fig. 3. Binding model of compound **10** (colored in green) into *E. coli* FabH (colored in blue). H-bond is shown as dotted green lines. π–π interaction is shown as yellow column (For interpretation of the references to colour in this figure legend, the reader is referred to the web version of this article.).

Phe 157. C1–N1–C8–C9 of compound **10** may form a hydrophobic interaction with Ile156, Phe304 and Met207 of *E. coli* FabH.

3. Conclusions

A series of novel Schiff bases reacting by 5-fluoro-salicylaldehyde and substituted primary amines were synthesized and assayed for their antibacterial activities against *E. coli*, *P. fluorescence*, *B. Subtilis* and *S. aureus*. Compound **10**, (*E*)-4-fluoro-2-((4-hydroxyphenethylimino)methyl)phenol showed the most potent antibacterial activity with MIC of 1.56–6.25 μg/mL against the test bacterial strains and exhibited the most potent *E. coli* FabH inhibitory activity with IC_{50} of 2.7 μM. The introduction of hydrophobic and electron-withdrawing halogeno groups was conducive to the antibacterial and *E. coli* FabH inhibitory activity. The introduction of tyramine into the Schiff base was favorable for the activity. Docking simulation was performed to position compound **10** into the *E. coli* FabH active site to determine the probable binding conformation.

4. Experimental section

4.1. Chemistry

All chemicals (reagent grade) used were commercially available. Melting points (uncorrected) were determined on a XT4 MP apparatus (Taike Corp., Beijing, China). ESI mass spectra were obtained on a Mariner System 5304 mass spectrometer, and ^{1}H NMR spectra were recorded on a Bruker PX500 or DPX300 spectrometer at 25 °C with TMS and solvent signals allotted as internal standards. Chemical shifts were reported in ppm (δ). Elemental analyses were performed on a CHN–O-Rapid instrument and were within ±0.4% of the theoretical values.

4.2. General method of synthesis of Schiff bases

Equimolar quantities (0.5 mmol) of 5-fluoro-salicylaldehyde and the substituted amines with one amino group were dissolved in methanol (10 mL) and stirred at room temperature for several hours. The precipitates were separated by filtration, recrystallized from methanol, washed with methanol for three times, and dried in a vacuum desiccator containing anhydrous $CaCl_2$.

4.2.1. (E)-2-((Cyclopentylimino)methyl)-4-fluorophenol (**1**)

Yellow oil, yield 85%, ^{1}H NMR (500 MHz, $CDCl_3$, δ, ppm): 1.60–1.63 (m, 4H); 1.72–1.76 (m, 2H); 1.93–1.95 (m, 2H); 3.92–3.96 (m, 1H); 6.85–6.88 (m, 1H); 6.99–7.01 (m, 1H); 7.04 (d, J = 3.0 Hz, 1H); 8.28 (s, 1H); 13.46 (s, 1H). MS (ESI): 208.13 ($C_{12}H_{15}FNO^+$, $[M + H]^+$). Anal. Calcd for $C_{12}H_{14}FNO$: C, 69.55%; H, 6.81%; N, 6.76%. Found: C, 69.72%; H, 6.84%; N, 6.75%.

4.2.2. (E)-4-Fluoro-2-((cyclohexylimino)methyl)phenol (**2**)

Yellow oil, yield 84%, ^{1}H NMR (500 MHz, $CDCl_3$, δ, ppm): 1.41–1.80 (m, 10H); 3.38–3.40 (m, 1H); 6.88–6.91 (m, 1H); 6.98 (dd, J = 3.0, 8.5 Hz, 1H); 7.06 (d, J = 3.0 Hz, 1H); 8.25 (s, 1H); 13.47 (s, 1H). ESI-MS: 222.12 ($C_{13}H_{17}FNO^+$, $[M + H]^+$). Anal. Calcd for $C_{13}H_{16}FNO$: C, 70.56%; H, 7.29%; N, 6.33%. Found: C, 70.47%; H, 7.82%; N, 6.32%.

4.2.3. (E)-2-((Cyclohexylmethylimino)methyl)-4-fluorophenol (**3**)

Yellow powder, yield 87%, mp: 36–37 °C, ^{1}H NMR (500 MHz, $CDCl_3$, δ, ppm): 1.00–1.07 (m, 2H); 1.16–1.28 (m, 3H); 1.66–1.68 (m, 2H); 1.73–1.78 (m, 4H); 3.45 (d, J = 6.3 Hz, 2H); 6.88–6.92 (m, 1H); 6.94 (d, J = 3.0 Hz, 1H); 7.01 (d, J = 3.0 Hz, 1H); 8.23 (s, 1H); 13.41 (s, 1H). MS (ESI): 236.13 ($C_{14}H_{19}FNO^+$, $[M + H]^+$). Anal. Calcd for $C_{14}H_{18}FNO$: C, 71.46%; H, 7.71%; N, 5.95%; Found: C, 71.35%; H, 7.74%; N, 5.93%.

4.2.4. (E)-4-Fluoro-2-((2-morpholinoethylimino)methyl)phenol (**4**)

Yellow oil, yield 89%, ^{1}H NMR (500 MHz, $CDCl_3$, δ, ppm): 2.53 (t, J = 4.6 Hz, 4H); 2.70 (t, J = 6.7 Hz, 2H); 3.71 (t, J = 4.7 Hz, 4H); 3.74 (t, J = 6.6 Hz, 2H); 6. 90 (t, J = 4.5 Hz, 1H); 6.94 (dd, J = 3.0, 8.4 Hz, 1H); 7.02 (d, J = 3.1 Hz, 1H); 8.30 (s, 1H); 13.10 (s, 1H). MS (ESI): 253.12 ($C_{13}H_{18}FN_2O_2^+$, $[M + H]^+$). Anal. Calcd for $C_{13}H_{17}FN_2O_2$: C, 61.89%; H, 6.79%; N, 11.10%; Found: C, 62.11%; H, 6.76%; N, 11.08%.

4.2.5. (E)-4-Fluoro-2-((3-morpholinopropylimino)methyl)phenol (**5**)

Yellow oil, yield 89%, ^{1}H NMR (500 MHz, $CDCl_3$, δ, ppm):1.86–1.91 (m, 2H); 2.41–2.44 (m, 6H); 3.66 (t, J = 6.7 Hz, 2H); 3.71 (t, J = 4.6 Hz, 4H); 6.85 (d, J = 9.3 Hz, 1H); 7.34–7.38 (m, 2H); 8.28 (s, 1H); 13.51 (s, 1H). MS (ESI): 267.15 ($C_{14}H_{20}FN_2O_2^+$, $[M + H]^+$). Anal. Calcd for $C_{14}H_{19}FN_2O_2$: C, 63.14%; H, 7.19%; N, 10.52%; Found: C, 63.28%; H, 7.15%; N, 10.49%.

4.2.6. (E)-4-Fluoro-2-((2-(piperazin-1-yl)ethylimino)methyl) phenol (**6**)

Yellow oil, yield 74%, ^{1}H NMR (500 MHz, $CDCl_3$, δ, ppm): 2.46–2.80 (m, 10H); 3.78 (t, J = 6.7 Hz, 2H); 6. 89 (t, J = 4.5 Hz, 1H); 6.94 (m, 1H); 7.04 (d, J = 3.2 Hz, 1H); 8.32 (s, 1H); 13.21 (s, 1H). MS (ESI): 252.2 ($C_{13}H_{19}FN_3O^+$, $[M + H]^+$). Anal. Calcd for $C_{13}H_{18}FN_3O$: C, 62.13%; H, 7.22%; N, 16.72%. Found: C, 62.28%; H, 7.24%; N, 16.78%.

4.2.7. (E)-2-((1-Benzylpiperidin-4-ylimino)methyl)-4-fluorophenol (**7**)

Yellow powder, yield 89%, mp: 93–95 °C, ^{1}H NMR (500 MHz, $CDCl_3$, δ, ppm): 1.83–1.86 (m, 4H); 2.22 (t, J = 5.6 Hz, 2H); 2.88 (d, J = 11.6 Hz, 2H); 3.30–3.32 (m, 1H); 3.53 (d, J = 12.6 Hz, 2H); 6.88–6.95 (m, 2H); 7.01 (d, J = 2.6 Hz, 1H); 7.26–7.35 (m, 5H); 8.32 (s, 1H); 13.25 (s, 1H). MS (ESI): 313.15 ($C_{19}H_{22}FN_2O^+$, $[M + H]^+$). Anal. Calcd for $C_{19}H_{21}FN_2O$: C, 73.05%; H, 6.78%; N, 8.97%; Found: C, 73.26%; H, 6.75%; N, 9.01%.

4.2.8. (E)-2-((3-(Dimethylamino)propylimino)methyl)-4-fluorophenol (**8**)

Yellow oil, yield 86%, ^{1}H NMR (500 MHz, $CDCl_3$, δ, ppm): 1.86–1.92 (m, 2H); 2.26 (s, 6H); 2.39 (t, J = 7.0 Hz, 2H); 3.66 (d,

J = 6.7 Hz, 2H); 6.90 (dd, J = 9.2, 4.6 Hz, 1H); 6.95 (dd, J = 8.3, 3.1 Hz, 1H); 7.00–7.04 (m, 1H); 8.30 (s, 1H); 13.23 (s, 1H). MS (ESI): 225.15 ($C_{12}H_{18}FN_2O^+$, $[M + H]^+$). Anal. Calcd for $C_{12}H_{17}FN_2O$: C, 64.26%; H, 7.64%; N, 12.49%; Found: C, 64.34%; H, 7.66%; N, 12.45%.

*4.2.9. (E)-2-((3-(Diethylamino)propylimino)methyl)-4-fluorophenol (**9**)*

Yellow oil, yield 87%, ^{1}H NMR (500 MHz, $CDCl_3$, δ, ppm): 1.02 (t, J = 7.2 Hz, 6H); 1.83–1.88 (m, 2H); 2.50–2.56 (m, 6H); 3.65 (t, J = 6.8 Hz, 2H); 6.89 (dd, J = 4.6, 8.9 Hz, 1H); 6.93–6.95 (m, 1H); 6.99–7.03 (m, 1H); 8.30 (s, 1H); 13.28 (s, 1H). MS (ESI): 253.14 ($C_{14}H_{22}FN_2O^+$, $[M + H]^+$). Anal. Calcd for $C_{14}H_{21}FN_2O$: C, 66.64%; H, 8.39%; N, 11.10%; Found: C, 66.78%; H, 8.36%; N, 11.07%.

*4.2.10. (E)-4-Fluoro-2-((4-hydroxyphenethylimino)methyl)phenol (**10**)*

Yellow crystals, yield 83%, mp: 161–163 °C, ^{1}H NMR (500 MHz, $CDCl_3$, δ, ppm): 2.93 (t, J = 7.1 Hz, 2H); 3.81 (t, J = 7.0 Hz, 2H); 6.75 (d, J = 8.6 Hz, 2H); 6.86–6.90 (m, 2H); 6.99–7.02 (m, 1H); 7.06 (d, J = 8.2 Hz, 2H); 8.12 (s, 1H); 8.90 (s, 1H); 13.48 (s, 1H). MS (ESI): 260.12 ($C_{15}H_{15}FNO_2^+$, $[M + H]^+$). Anal. Calcd for $C_{15}H_{14}FNO_2$: C, 69.49%; H, 5.44%; N, 5.40%; Found: C, 69.63%; H, 5.46%; N, 5.37%.

*4.2.11. (E)-2-Fluoro-6-((p-tolylimino)methyl)phenol (**11**)*

Yellow powder, yield 88%, mp: 128–130 °C, ^{1}H NMR (300 MHz, $CDCl_3$, δ, ppm): 2.36 (s, 3H); 6.81–6.88 (m, 1H); 7.15 (d, J = 1.5 Hz, 1H); 7.18–7.19 (m, 1H); 7.21–7.23 (m, 4H); 8.64 (s, 1H); 13.74 (s, 1H); MS (ESI): 230.09 ($C_{14}H_{13}FNO^+$, $[M + H]^+$). Anal. Calcd for $C_{14}H_{12}FNO$: C, 73.35%; H, 5.28%; N, 6.11%; Found: C, 73.38%; H, 5.26%; N, 6.12%.

*4.2.12. (E)-2-Fluoro-6-((4-isopropylphenylimino)methyl)phenol (**12**)*

Yellow crystals, yield 93%, mp: 64–65 °C, ^{1}H NMR (300 MHz, $CDCl_3$, δ, ppm): 1.27 (d, J = 4.0 Hz, 3H); 1.32 (d, J = 4.2 Hz, 3H); 2.99 (m, 1H); 6.87–6.91 (m, 1H); 7.14 (d, J = 1.5, 1H); 7.18–7.19 (m, 1H); 7.29 (d, J = 7.2 Hz, 2H); 7.30 (s, 1H); 7.34 (d, J = 7.0 Hz, 2H); 8.69 (s, 1H); 13.77 (s, 1H); MS (ESI): 258.12 ($C_{16}H_{17}FNO^+$, $[M + H]^+$). Anal. Calcd for $C_{16}H_{16}FNO$: C, 74.69%; H, 6.27%; N, 5.44%; Found: C, 74.65%; H, 6.28%; N, 5.42%.

*4.2.13. (E)-2-Fluoro-6-((4-fluorophenylimino)methyl)phenol (**13**)*

Yellow powder, yield 76%, mp: 127–129 °C, ^{1}H NMR (300 MHz, $CDCl_3$, δ, ppm): 6.83–6.90 (m, 1H); 7.09–7.22 (m, 4H); 7.27–7.30 (m, 2H); 8.61 (s, 1H); 13.40 (s, 1H); MS (ESI): 234.07 ($C_{13}H_{10}F_2NO^+$, $[M + H]^+$). Anal. Calcd for $C_{13}H_9F_2NO$: C, 66.95%; H, 3.89%; N, 6.01%; Found: C, 66.91%; H, 3.90%; N, 6.03%.

*4.2.14. (E)-2-((4-Chlorophenylimino)methyl)-6-fluorophenol (**14**)*

Yellow powder, yield 87%, mp: 129–131 °C, ^{1}H NMR (500 MHz, $CDCl_3$, δ, ppm): 6.86–6.90(m, 1H); 7.19 (d, J = 7.3 Hz, 2H); 7.23 (d, J = 8.6 Hz, 2H); 7.40 (s, 1H); 7.41 (s, 1H); 8.62 (s, 1H); 13.28 (s, 1H); MS (ESI): 251.03 ($C_{13}H_{10}ClFNO^+$, $[M + H]^+$). Anal. Calcd for $C_{13}H_9ClFNO$: C, 62.54%; H, 3.63%; N, 5.61%; Found: C, 62.52%; H, 3.65%; N, 5.62%.

*4.2.15. (E)-2-((4-Bromophenylimino)methyl)-6-fluorophenol (**15**)*

Yellow powder, yield 89%, mp: 148–149 °C, ^{1}H NMR (300 MHz, $CDCl_3$, δ, ppm): 6.95–6.99 (m, 1H); 7.17 (d, J = 8.6 Hz, 2H); 7.19 (d, J = 8.7 Hz, 2H); 7.54 (s, 1H); 7.57 (s, 1H); 8.62 (s, 1H); 13.27 (s, 1H); MS (ESI): 293.99 ($C_{13}H_{10}BrFNO^+$, $[M + H]^+$). Anal. Calcd for $C_{13}H_9BrFNO$: C, 53.09%; H, 3.08%; N, 4.76%; Found: C, 53.06%; H, 3.10%; N, 4.72%.

*4.2.16. (E)-2-Fluoro-6-((4-hydroxyphenylimino)methyl)phenol (**16**)*

Yellow crystals, yield 89%, mp: 168–170 °C, ^{1}H NMR (500 MHz, $CDCl_3$, δ, ppm): 6.87–6.90 (m, 1H); 6.94 (d, J = 8.5 Hz, 2H); 7.19–7.23 (m, 2H); 7.29 (d, J = 8.8 Hz, 2H); 8.66 (s, 1H); 13.76 (s, 1H); MS (ESI): 232.07 ($C_{13}H_{11}FNO_2^+$, $[M + H]^+$). Anal. Calcd for $C_{13}H_{10}FNO_2$: C, 67.53%; H, 4.36%; N, 6.06%; Found: C, 67.52%; H, 4.38%; N, 6.08%.

*4.2.17. (E)-4-fluoro-2-((4-nitrophenylimino)methyl)phenol (**17**)*

Yellow crystals, yield 85%, mp: >200 °C, ^{1}H NMR (500 MHz, $CDCl_3$, δ, ppm): 7.07 (d, J = 8.6 Hz, 1H); 7.54–7.60 (m, 3H); 7.85–7.87 (m, 1H); 8.34 (d, J = 8.7 Hz, 2H); 8.64 (s, 1H); 13.53 (s, 1H); MS (ESI): 261.05 ($C_{13}H_{10}FN_2O_3^+$, $[M + H]^+$). Anal. Calcd for $C_{13}H_9FN_2O_3$: C, 60.00%; H, 3.49%; N, 10.77%; Found: C, 60.23%; H, 3.46%; N, 10.79%.

*4.2.18. (E)-2-Fluoro-6-((2-fluorophenylimino)methyl)phenol (**18**)*

Yellow crystals, yield 86%, mp: 111–112 °C, ^{1}H NMR (300 MHz, $CDCl_3$, δ, ppm): 7.18–7.30 (m, 7H); 8.74 (s, 1H); 13.40 (s, 1H); MS (ESI): 234.07 ($C_{13}H_{10}F_2NO^+$, $[M + H]^+$). Anal. Calcd for $C_{13}H_9F_2NO$: C, 66.95%; H, 3.89%; N, 6.01%; Found: C, 66.92%; H, 3.90%; N, 6.03%.

*4.2.19. (E)-2-((2-Chlorophenylimino)methyl)-6-fluorophenol (**19**)*

Yellow powder, yield 86%, mp: 100–104 °C, ^{1}H NMR (300 MHz, $CDCl_3$, δ, ppm): 7.19–7.28 (m, 5H); 7.33 (d, J = 7.4 Hz, 1H); 7.50 (d, J = 7.8 Hz, 1H); 13.45 (s, 1H); MS (ESI): 250.04 ($C_{13}H_{10}ClFNO^+$, $[M + H]^+$). Anal. Calcd for $C_{13}H_9ClFNO$: C, 62.54%; H, 3.63%; N, 5.61%; Found: C, 62.52%; H, 3.66%; N, 5.63%.

*4.2.20. (E)-4-Fluoro-2-((pyridin-2-ylimino)methyl)phenol (**20**)*

Yellow crystal, yield 85%, mp: 94–95 °C, ^{1}H NMR (300 MHz, $CDCl_3$, δ, ppm): 6.96–7.00 (m, 1H); 7.09–7.22 (m, 4H); 7.33 (d, J = 7.9 Hz, 1H); 7.79 (t, J = 7.9 Hz, 1H); 8.51–8.52 (m, 1H); 9.39 (s, 1H); 13.20 (s, 1H); MS (ESI): 217.06 ($C_{12}H_{10}FN_2O^+$, $[M + H]^+$). Anal. Calcd for $C_{12}H_9FN_2O$: C, 66.66%; H, 4.20%; N, 12.96%; Found: C, 66.82%; H, 4.18%; N, 13.01%.

4.3. Crystal structure determination

Crystal structure determination of compound **10** was carried out on a Nonius CAD4 diffractometer equipped with graphite-monochromated MoKα (λ = 0.71073 Å) radiation. The structure was solved by direct methods and refined on F^2 by full-matrix least-squares methods using SHELX-97 [31]. All the non-hydrogen atoms were refined anisotropically. All the hydrogen atoms were placed in calculated positions and were assigned fixed isotropic thermal parameters at 1.2 times the equivalent isotropic U of the atoms to which they are attached and allowed to ride on their respective parent atoms. The contributions of these hydrogen atoms were included in the structure-factors calculations. The crystal data, data collection, and refinement parameter for the compound **10** are listed in Table 3.

4.4. Antibacterial activity

The antibacterial activity of the synthesized compounds was tested against *E. coli*, *P. fluorescence*, *B. subtilis* and *S. aureus* using MH medium (Mueller–Hinton medium: casein hydrolysate 17.5 g, soluble starch 1.5 g, beef extract 1000 mL), The MICs (minimum inhibitory concentrations) of the test compounds were determined by a colorimetric method using the dye MTT (3-(4,5-dimethylthiazol-2-yl)-2,5-diphenyl trtrazolium bromide). A stock solution of the synthesized compound (100 μg/mL) in DMSO was prepared and graded quantities of the test compounds were incorporated in specified quantity of sterilized liquid MH medium. A specified quantity of the medium containing the compound was poured into microtitration plates. Suspension of the microorganism was prepared to contain approximately 10^5 cfu/mL and applied to

Table 3
Crystallographical and experimental data for compound **10**.

Compound	**10**
Formula	$C_{15}H_{14}FNO_2$
Mr (Formula weight)	259.27
Crystal system	Monoclinic
Space group	*C*2/*c*
a (Å)	15.979(3)
b (Å)	12.941(3)
c (Å)	15.040(3)
α (°)	90
β (°)	121.72(3)
γ (°)	90
Volume (Å^3)	2645.5(9)
Z (formula units)	8
Dc/(g/cm^3) (Calculated density)	1.302
μ (mm^{-1})[a]	0.096
F(000)[b]	1088
Crystal size (mm^3)	0.35 × 0.30 × 0.30
T/*K* (Data collection temperature)	293(2)
θ range/°	2.17/25.96
Index ranges	0<=*h*<=19 0<=*k*<=15 −18<=*l*<=15
Reflections collected/unique	2692/2599 [R(int) = 0.0518]
Observed reflections	1431
Data/restraints/parameters	2599/0/176
Goodness-of-fit on F^2	1.021
Final *R* indices [$I \geq 2\sigma(I)$][c]	$R_1 = 0.0659$, $\omega R_2 = 0.1524$
R indices (all data)[c]	$R_1 = 0.1223$, $\omega R_2 = 0.1868$
Largest diff. peak and hole (eÅ^{-3})	0.305 and −0.225

[a] Absorption coefficient.
[b] The number of electrons in a single cell.
[c] $R_1 = \Sigma||Fo| - |Fc||/\Sigma|Fo|$, $wR_2 = [\Sigma w(Fo^2 - Fc^2)^2/\Sigma w(Fo^2)^2]^{1/2}$.

microtitration plates with serially diluted compounds in DMSO to be tested and incubated at 37 °C for 24 h. After the MICs were visually determined on each of the microtitration plates, 50 μL of PBS (Phosphate Buffered Saline 0.01 mol/L, pH 7.4: $Na_2HPO_4.12H_2O$ 2.9 g, KH_2PO_4 0.2 g, NaCl 8.0 g, KCl 0.2 g, distilled water 1000 mL) containing 2 mg of MTT/mL was added to each well. Incubation was continued at room temperature for 4–5 h. The content of each well was removed, and 100 μL of isopropanol containing 5% 1 mol/L HCl was added to extract the dye. After 12 h of incubation at room temperature, the optical density (OD) was measured with a microplate reader at 550 nm. The observed MICs were presented in Table 1.

4.5. *E. coli* FabH purification and activity assay

Full-length *E. coli* acyl carrier protein (ACP), acyl carrier protein synthase (ACPS), and β-ketoacyl-ACP synthase III (FabH) were individually cloned into pET expression vectors with an N-terminal His-tag (ACP, ACPS in pET19; FabH in pET28).

All proteins were expressed in *E. coli* strain BL21(DE3). Transformed cells were grown on Luria-Bertani (LB) agar plates supplemented with kanamycin (30 μg/ml). Sodium dodecyl sulfate-polyacrylamide gel electrophoresis (SDS-PAGE) analysis was used to screen colonies for overexpression of proteins. One such positive colony was used to inoculate 10 ml of LB medium with 30 μg/ml of kanamycin and grown overnight at 37 °C, 1 ml of which was used to inoculate 100 ml LB medium supplemented with 30 μg/ml of kanamycin. The culture was shaken for 4 h at 37 °C, and then induced with 0.5 mM isopropyl β-D-thiogalactopyranoside (IPTG). The culture was grown for 4 h, and harvested by centrifugation (30 min at 15 000 rpm).

Harvested cells containing His-tagged ACP, ACPS, and FabHs were lysed by sonication in 20 mM Tris, pH 7.6, 5 mM imidazole, 0.5 M NaCl and centrifuged at 20,000 rpm for 30 min. The supernatant was applied to a Ni-NTA agarose column, washed, and eluted using a 5–500 mM imidazole gradient over 20 column volumes. Eluted protein was dialyzed against 20 mM Tris, pH 7.6, 1 mM DTT, and 100 mM NaCl. Purified FabHs were concentrated up to 2 mg/mL and stored at −80 °C in 20 mM Tris, pH 7.6, 100 mM NaCl, 1 mM DTT, and 20% glycerol for enzymatic assays.

Purified ACP contains the apo-form that needs to be converted into the holo-form. The conversion reaction is catalyzed by ACP synthase (ACPS). In the final volume of 50 mL, 50 mg ACP, 50 mM Tris, 2 mM DTT, 10 mM MgCl2, 600 μM CoA, and 0.2 μM ACPS was incubated for 1 h at 37 °C. The pH of the reaction was then adjusted to approximately 7.0 using 1 M potassium phosphate. Holo-ACP was purified by fractionation of the reaction mixture by Source Q-15 ion exchange chromatography using a 0–500 mM NaCl gradient over 25 column volumes.

In a final 20 μL reaction, 20 mM Na_2HPO_4/NaH_2PO_4, pH 7.0, 0.5 mM DTT, 0.25 mM $MgCl_2$, and 2.5 μM holo-ACP were mixed with 1 nM FabH, and H_2O was added to 15 μL. After 1 min incubation, a 2 μL mixture of 25 μM acetyl-CoA and 0.75 μCi [^{3}H]acetyl-CoA was added for FabH reaction for 25 min. The reaction was stopped by adding 20 μL of ice-cold 50% TCA, incubating for 5 min on ice, and centrifuging to pellet the protein. The pellet was washed with 10% ice-cold TCA and resuspended with 5 μL of 0.5 M NaOH. The incorporation of the ^{3}H signal in the final product was read by liquid scintillation. When determining the inhibition constant (IC_{50}), inhibitors were added from a concentrated DMSO stock such that the final concentration of DMSO did not exceed 2%.

4.6. Docking simulations

The crystal structures of *E. coli* FabH (PDB code: 1HNJ) [30] was obtained from the Protein Data Bank (http://www.rcsb.org).

Studies were carried out on only one subunit of the enzymes. The graphical user interface AutoDockTools (ADT) was employed to setup the enzymes: all hydrogens were added, Gasteiger charges were calculated and nonpolar hydrogens were merged to carbon atoms. For macromolecules, generated pdbqt files were saved.

The 3D structures of ligand molecules were built, optimized (PM3) level, and saved in mol2 format with the aid of the molecular modeling program Spartan (Wavefunction Inc.). These partial charges of Mol2 files were further modified by using the ADT package (version 1.4.6) so that the charges of the nonpolar hydrogens atoms assigned to the atom to which the hydrogen is attached. The resulting files were saved as pdbqt files.

AutoDock 4.0 was employed for all docking calculations [32,33]. The AutoDockTools program was used to generate the docking input files. In all docking a grid box size of 48 × 48 × 48 points in x, y, and z directions was built in the catalytic site of the protein. A grid spacing of 0.375 Å (approximately one forth of the length of carbon–carbon covalent bond) and a distances-dependent function of the dielectric constant were used for the calculation of the energetic map. Ten runs were generated by using Lamarckian genetic algorithm searches. Default settings were used with an initial population of 50 randomly placed individuals, a maximum number of 2.5×10^6 energy evaluations, and a maximum number of 2.7×10^4 generations. A mutation rate of 0.02 and a crossover rate of 0.8 were chosen. Results differing by less than 0.5 Å in positional root-mean-square deviation (RMSD) were clustered together and the results of the most favorable free energy of binding were selected as the resultant complex structures.

Acknowledgements

This work was supported by the Jiangsu National Science Foundation (No. BK2009239) and Anhui National Science Foundation (No. 070416274X).

References

[1] M. Leeb, Nature 431 (2004) 892–893.
[2] J.E. Cronan Jr., C.O. Rock, in: F.C. Neidhardt, I.L. Ingraham, K.B. Low, et al. (Eds.), *Escherichia coli* and *Salmonella typhimurium*: Cellular and Molecular Biology, American Society of Microbiology, Washington, DC, 1996, pp. 612–638.
[3] C.Y. Lai, J.E. Cronan, J. Biol. Chem. 19 (2003) 51494–51503.
[4] Y.J. Lu, Y.M. Zhang, C.O. Rock, Biochem. Cell Biol. 82 (2004) 145–155.
[5] A. Jayakumar, M.-H. Tai, W.-Y. Huang, W. Al-Feel, M. Hsu, L. Abu-Elheiga, S. Chirala, S. Wakil, J. Proc. Natl. Acad. Sci. USA 92 (1995) 8695–8699.
[6] S.W. White, J. Zheng, Y.M. Zhang, C.O. Rock, Annu. Rev. Biochem 74 (2005) 791–831.
[7] R. Veyron-Churlet, O. Guerrini, L. Mourey, M. Daffé, D. Zerbib, Mol. Microbiol. 54 (2004) 1161–1172.
[8] S.S. Khandekar, R.A. Daines, J.T. Lonsdale, Curr. Protein Pept. Sci. 4 (2003) 21–29.
[9] R.J. Heath, C.O. Rock, Nat. Prod. Rep. 19 (2002) 581–596.
[10] J.T. Tsay, W. Oh, T.J. Larson, S. Jakowski, C.O. Rock, J. Biol. Chem. 267 (1992) 6807–6814.
[11] R.C. Clough, A.L. Matthis, S.R. Barnum, J.G. Jaworski, J. Biol. Chem. 267 (1992) 20992–20998.
[12] R.J. Heath, C.O. Rock, J. Biol. Chem. 271 (1996) 1833–1836.
[13] C.E. Christensen, B.B. Kragelund, P. von Wettstein-Knowles, A. Henriksen, Protein Sci. 16 (2007) 261–272.
[14] W. Bylka, I. Matlawska, N.A. Pilewski, JANA 7 (2004) 24–31.
[15] M.M. Huycke, D.F. Sahm, M.S. Gilmore, Emergen. Infect. Dis. 4 (1998) 239–249.
[16] R. Puupponen-Pimi, L. Nohynek, C. Meier, M. Kähkönen, A.H. Heinonen, J. Appl. Microbiol. 90 (2001) 494–507.
[17] X. Qiu, C.A. Janson, A.K. Konstantinidis, S. Nwagwu, C. Silverman, W.W. Smith, S. Khandekar, J. Lonsdale, S.S. Abdel-Meguid, J. Biol. Chem. 274 (1999) 36465–36471.
[18] B. Vladimir, P. Nikolai, Exp. Rev. Clin. Immunol. 1 (2005) 145–157.
[19] P.J. Lee, J.B. Bhonsle, H.W. Gaona, D.P. Huddler, T.N. Heady, M. Kreishman-Deitrick, A. Bhattacharjee, W.F. McCalmont, L. Gerena, M. Lopez-Sanchez, N.E. Roncal, T.H. Hudson, J.D. Johnson, S.T. Prigge, N.C. Waters, J. Med. Chem. 52 (2009) 952–963.
[20] Z. Nie, C. Perretta, J. Lu, Y. Su, S. Margosiak, K.S. Gajiwala, J. Cortez, V. Nikulin, K.M. Yager, K. Appelt, S. Chu, J. Med. Chem. 48 (2005) 1596–1609.
[21] R.A. Daines, I. Pendrak, K. Sham, G.S.V. Aller, A.K. Konstantinidis, J.T. Lonsdale, C.A. Janson, X. Qiu, M. Brandt, S.S. Khandekar, C. Silverman, M.S. Head, J. Med. Chem. 46 (2003) 5–8.
[22] A. Asheka, S.J. Cho, Bioorg. Med. Chem. 14 (2006) 1474–1482.
[23] S. Singh, L.K. Soni, M.K. Gupta, Y.S. Prabhakar, S.G. Kaskhedikar, Eur. J. Med. Chem. 43 (2008) 1071–1080.
[24] J.-Y. Lee, K.-W. Jeong, J.-U. Lee, D.-I. Kang, Y. Kim, Bioorg. Med. Chem. 17 (2009) 1506–1513.
[25] A. Ito, K. Hirai, M. Inoue, H. Koga, S. Suzue, T. Irikura, S. Mitsuhashi, Antimicrob. Agents. Chemother. 17 (1980) 103–108.
[26] M. Calas, J. Bompart, L. Giral, G. Grassy, Eur. J. Med. Chem. 26 (1991) 279–290.
[27] Y. Kotera, Y. Inoue, M. Ohashi, K. Ito, G. Tsukamoto, Chem. Pharm. Bull. 39 (1991) 2644–2646.
[28] M.C. Bagchi, D. Mills, S.C. Basak, J. Mol. Model. 13 (2007) 111–120.
[29] F.H. Allen, O. Kennard, D.G. Watson, L. Brammer, A.G. Orpen, R.J. Taylor, Chem. Soc. Perkin Trans. 2 (1987) S1–S19.
[30] X. Qiu, C.A. Janson, W.W. Smith, M. Head, J. Lonsdale, A.K. Konstantinidis, J. Mol. Biol. 307 (2001) 341–356.
[31] G.M. Sheldrick, Acta. Crystallogr. A64 (2008) 112–122.
[32] G.M. Morris, D.S. Goodsell, R.S. Halliday, R. Huey, W.E. Hart, R.K. Belew, A.J. Olson, J. Comput. Chem. 19 (1998) 1639–1662.
[33] R. Huey, G.M. Morris, A.J. Olson, D.S. Goodsell, J. Comput. Chem. 28 (2007) 1145–1152.